

ICSV14

Cairns • Australia

9-12 July, 2007



VIBRATIONS OF MULTI-SPAN BRIDGES UNDER MOVING LOADS

Hongan Xu and Wen L. Li

Department of Mechanical Engineering
Mississippi State University
Mississippi State, MS 39762, USA
li@me.msstate.edu

Abstract

This study is concerned with the dynamic behavior of generic multi-span bridges under a concentrated moving load. In this multi-span bridge model, each span can be independently supported by up to eight elastic springs, thus allowing a more general and realistic representation of many joints and intermediate supports of practical concern. Additionally, since the displacement and its first derivative are no longer required to be continuous at an intermediate support, this model is capable of accounting for the vehicle-bridge interactions resulting from the possible steps and skew angles at the span junctions. Numerical results are presented with a focus on the dynamic impact of the coupling conditions between spans. It has been shown that the deflection on each span strongly depend upon its local coupling conditions, especially near the critical stiffness values defined by the bending rigidities of the involved beams. A fairly large variance of response has also been observed on each span in correspondence to a wide range of stiffness values, which implies a good potential for improving bridge performance through varying joint stiffnesses and/or coupling configurations. This analysis method can be readily applied to any boundary and coupling conditions with no need of changing or modifying the formulations or solution procedures.

1. INTRODUCTION

The dynamic behavior of multi-span beams under moving loads has been extensively studied for many years in connection with the design of railway tracks and bridges. Although a grid-based solution method may be considered inconvenient in dealing with the problems involving moving loads, the finite element method is still one of the most powerful numerical methods and used by many researchers [1-3]. Dynamic stiffness based method is another popular technique for the vibrations of beams subjected to moving loads [4-7]. Henchi and Fafard [4] derived the frequencies and mode shapes of a uniform continuous beam by using the dynamic stiffness element method under the framework of finite element approximation. Dugush and Eisenberger [7] presented a solution for the multi-span non-uniform beams transversely by a load traveling at a constant or variable velocity. The assumed mode method

is also widely used to solve single- and multi-span beam problems [8-13]. Ichikawa and Miyakawa [12] gave a solution for a uniform continuous beam under a concentrated load moving at variable velocity. The solution was based on the mode superposition method and the final system equations in the case of variable velocity were solved numerically using the central difference method. Zheng *et al.* [13, 14] studied the vibration of a multi-span non-uniform beam using the modified beam vibration functions as the assumed modes. Other commonly used methods include Laplace transformations [15-18], the methods of Lagrange multipliers [19-21], the Green's function methods [22-26], and so on.

Many of the aforementioned methods will require a varying degree of modifications or adaptations to account for the variances in boundary conditions, intermediate supports, and/or the number of spans. For instance, when the unconstrained beam functions are used as the assume mode shapes, one typically needs to first determine the eigenfunctions for the given boundary conditions. This problem itself may become a sizeable task if the beam is elastically restrained at either or both ends. In addition, the beam eigenfunctions tend to become numerically unstable for large modal indexes, which demands special treatments in actual calculations.

In most investigations, the term “multi-span beams” typically refers to a continuous beam with a number of intermediate supports. Although the beams may be allowed to have different physical or geometrical properties for each span, the beam displacement and its first derivatives are required to be continuous over the entire beam length. This condition can be easily violated when the translational and rotational couplings between any two adjacent spans are not sufficiently strong to ensure a smooth transition of the displacement and its derivative at the junction. Many modern structures such as bridges, railroad tracks, and pipelines are assembled from some fundamental building blocks through joints. Thus, it is important to extend the definition of multi-span beam to include a beam system comprising a number of beams co-linearly coupled together via rigid and non-rigid joints. Accordingly, at the junctions the kinematic continuity requirements on the displacement function will need to be replaced with the dynamic equilibrium equations about the forces and moments.

A modified Fourier series method was recently developed by Li *et al.* for determining the vibration of a single beam with elastic boundary supports [27] and the vibratory energy flows between two beams coupled elastically via a set of linear and rotational springs [28, 29]. This method was later extended to the free vibrations of multi-span beam systems. In this investigation, we will study the dynamic response of a multi-span bridge to a moving load with emphasizing on the effects of the between-span coupling conditions. Substantial insightful information has been gained through numerical simulations regarding how to effectively modify or improve the dynamic behavior of a multi-span bridge.

2. DESCRIPTION OF THE ANALYSIS METHOD

Figure 1 shows a dynamic system which consists of multiple beams coupled together via a set of joints represented by linear and rotational springs. The elastic springs between any two adjacent beams allows considering the non-rigid effect of some practical joints such as bolts or point welds. The conventional rigid connectors can be considered as a special case when the stiffnesses of these springs become substantially larger than the bending rigidities of the beams. Each of beams may also be supported on a set of elastic restraints at both ends. All the traditional intermediate supports and homogeneous boundary conditions (*i.e.*, the combinations of the simply supported, free, guided and clamped end conditions) can be readily obtained from these general boundary conditions by accordingly setting the stiffness constants of the restraining springs to equal to zero or infinity.

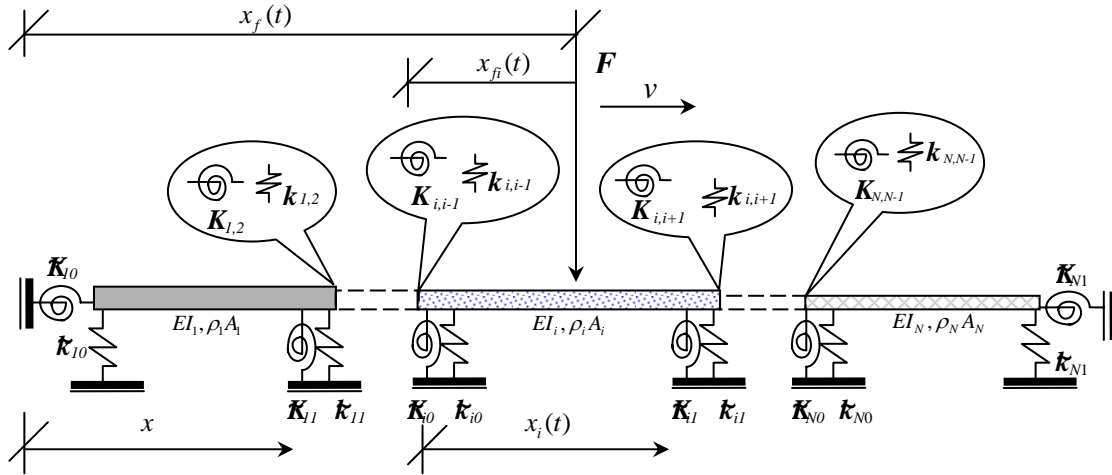


Figure 1. A multi-span bridge subjected to a concentrated moving load.

The differential equation for the vibration of the i -th beam is well known as

$$D_i d^4 w_i(x,t)/dx^4 - \rho_i A_i \omega^2 w_i(x,t) = F \delta(x - x_{fi}(t)) \quad (i = 1, 2, \dots, N) \quad (1)$$

where $w_i(x,t)$, D_i , ρ_i , and S_i are respectively the flexural displacement, the bending rigidity, the mass density and the cross-sectional area of i -th beam; ω is angular frequency and x represents the local co-ordinate measured from the left end of the i -th span; and F is the magnitude of the concentrated moving load, δ is the Dirac delta function, and $x_{fi}(t)$ ($x_f(t)$) is the load position measured from the left end of the i -th (first) beam.

In this paper, the load profile is defined by

$$\ddot{x}_f(t) = a = \text{constant}, \quad \dot{x}_f(t) = v = v_0 + at, \quad \text{and} \quad x_f(t) = v_0 t + at^2/2$$

where a is the acceleration of the moving load, $v = v(t)$ is its velocity, and v_0 is the initial velocity at time $t = 0$ when the load is just about to enter the first beam.

The boundary and coupling conditions for the i -th beam can be expressed as at $x = 0$,

$$k_{i,i-1}(w_i(x,t) - w_{i-1}(x,t)) + \tilde{k}_{i0} w_i(x,t) = -D_i w_i'''(x,t) \quad , \quad (2)$$

$$K_{i,i-1}(w_i'(x,t) - w_{i-1}'(x,t)) + \tilde{K}_{i0} w_i'(x,t) = D_i w_i''(x,t) \quad , \quad (3)$$

at $x = L_i$,

$$k_{i,i+1}(w_i(x,t) - w_{i+1}(x,t)) + \tilde{k}_{i1} w_i(x,t) = D_i w_i'''(x,t) \quad , \quad (4)$$

$$K_{i,i+1}(w_i'(x,t) - w_{i+1}'(x,t)) + \tilde{K}_{i1} w_i'(x,t) = -D_i w_i''(x,t) \quad , \quad (5)$$

at the left end (of the first beam),

$$\tilde{k}_{10} w_1(x,t) = -D_1 w_1'''(x,t), \quad \tilde{K}_{10} w_1'(x,t) = D_1 w_1''(x,t), \quad (6,7)$$

at the right end (of the N -th beam),

$$\tilde{k}_{N1}w_N(x,t) = D_N w_N'''(x,t), \quad \tilde{K}_{N1}w_N'(x,t) = -D_N w_N''(x,t), \quad (8,9)$$

where, refer to Fig. 1, $k_{i,j}$ and $K_{i,j}$ denote the stiffnesses of the linear and rotational springs at the junction of beams i and j , respectively; $\tilde{k}_{i,0}, \tilde{k}_{i,l}$ are the stiffnesses of linear springs, and $\tilde{K}_{i,0}, \tilde{K}_{i,l}$ the stiffnesses of the rotational springs at the left and right ends of beam i , respectively.

All the conventional homogeneous beam boundary conditions can be considered as the special cases of equations (6-9). For example, the simply supported end condition is easily modeled by simply setting the stiffnesses of the translational and rotational springs to be extremely large and small, respectively.

On each beam, the displacement will be sought in the form of

$$w_i(x,t) = \sum_{m=0}^{\infty} A_{i,m}(t) \cos \lambda_{i,m} x + p_i(x,t), \quad 0 \leq x \leq L_i \quad (\lambda_{i,m} = \frac{m\pi}{L_i}) \quad (10)$$

where L_i is the length of i -th beam.

In equation (10), an auxiliary function $p_i(x)$ was introduced to improve the accuracy and convergence of the series expansion at the end points, $x=0$ and L_i . It is specifically required to satisfy the following conditions:

$$p_i'''(0,t) = w_i'''(0,t) = \alpha_{i0}, \quad (11)$$

$$p_i'''(L_i,t) = w_i'''(L_i,t) = \alpha_{i1}, \quad (12)$$

$$p_i'(0,t) = w_i'(0,t) = \beta_{i0}, \quad (13)$$

$$p_i'(L_i,t) = w_i'(L_i,t) = \beta_{i1}. \quad (14)$$

The benefits for using such an auxiliary function were adequately discussed before in ref. [27] and will not be further elaborated here. Theoretically, the auxiliary function $p_i(x)$ can be any continuous closed-form function defined over $[0, L_i]$. As an example, the auxiliary function $p_i(x)$ will be here selected as a polynomial:

$$p_i = \zeta_i(x)^T \alpha_i \quad (15)$$

where

$$\alpha_i = \{\alpha_{i0}, \alpha_{i1}, \beta_{i0}, \beta_{i1}\}^T \quad (16)$$

and

$$\zeta_i(x)^T = \left\{ \begin{array}{l} -(15x^4 - 60L_i x^3 + 60L_i^2 x^2 - 8L_i^4)/360L_i \\ (15x^4 - 30L_i^2 x^2 + 7L_i^4)/360L_i \\ (6L_i x - 2L_i^2 - 3x^2)/6L_i \\ (3x^2 - L_i^2)/6L_i \end{array} \right\} \quad (17)$$

It should be pointed out that although the same symbol is used, the x -coordinate in equation (17) actually represents a local coordinate system with its origin at the left end of each beam. However, the use of different local coordinate systems is simply for the sake of mathematical convenience.

At this point, the auxiliary function is fully defined in terms of 4 unknown boundary constants, $\alpha_i = \{\alpha_{i0}, \alpha_{i1}, \beta_{i0}, \beta_{i1}\}^T$. In what follows, these unknowns will be determined as the functions of the Fourier coefficients.

Substituting equations (10-17) into equations (2-9) leads to

$$\begin{aligned}
 & k_{i,i-1} \left(\sum_{m=0}^{\infty} (-1)^m A_{i-1,m}(t) - \frac{7L_{i-1}^3 \alpha_{i-1,0}}{360} - \frac{8L_{i-1}^3 \alpha_{i-1,1}}{360} + \frac{\beta_{i-1,0} L_{i-1}}{6} + \frac{\beta_{i-1,1} L_{i-1}}{3} \right) \\
 &= D_i \alpha_{i,0} + (k_{i,i-1} + \tilde{k}_{i0}) \left(\sum_{m=0}^{\infty} A_{i,m}(t) + \frac{8L_i^3 \alpha_{i,0}}{360} + \frac{7L_i^3 \alpha_{i,1}}{360} - \frac{\beta_{i,0} L_i}{3} - \frac{\beta_{i,1} L_i}{6} \right) \quad (18)
 \end{aligned}$$

$$(K_{i,i-1} + \tilde{K}_{i0}) \beta_{i,0} = K_{i,i-1} \beta_{i-1,1} + D_i \left(- \sum_{m=1}^{\infty} \lambda_{i,m}^2 A_{i,m}(t) - \frac{\alpha_{i,0} L_i}{3} - \frac{\alpha_{i,1} L_i}{6} + \frac{\beta_{i,1}}{L_i} - \frac{\beta_{i,0}}{L_i} \right) \quad (19)$$

$$\begin{aligned}
 & (k_{i,i+1} + \tilde{k}_{i1}) \left(\sum_{m=0}^{\infty} (-1)^m A_{i,m}(t) - \frac{7L_i^3 \alpha_{i,0}}{360} - \frac{8L_i^3 \alpha_{i,1}}{360} + \frac{\beta_{i,0} L_i}{6} + \frac{\beta_{i,1} L_i}{3} \right) = \\
 & D_i \alpha_{i,1} + k_{i,i+1} \left(\sum_{m=0}^{\infty} A_{i+1,m}(t) + \frac{8L_{i+1}^3 \alpha_{i+1,0}}{360} + \frac{7L_{i+1}^3 \alpha_{i+1,1}}{360} - \frac{\beta_{i+1,0} L_{i+1}}{3} - \frac{\beta_{i+1,1} L_{i+1}}{6} \right) \quad (20)
 \end{aligned}$$

$$(K_{i,i+1} + \tilde{K}_{i1}) \beta_{i,1} = K_{i,i+1} \beta_{i+1,0} - D_i \left(\sum_{m=1}^{\infty} (-1)^{m+1} \lambda_{i,m}^2 A_{i,m}(t) + \frac{\alpha_{i,0} L_i}{6} + \frac{\alpha_{i,1} L_i}{3} + \frac{\beta_{i,1}}{L_i} - \frac{\beta_{i,0}}{L_i} \right). \quad (21)$$

In matrix form, the above equations simplifies to

$$\mathbf{H}_{i,i-1} \boldsymbol{\alpha}_{i-1} + \mathbf{H}_{i,i} \boldsymbol{\alpha}_i + \mathbf{H}_{i,i+1} \boldsymbol{\alpha}_{i+1} = \sum_{m=0}^{\infty} (\mathbf{Q}_{i,i-1}^m \mathbf{A}_{i-1,m}(t) + \mathbf{Q}_{i,i}^m \mathbf{A}_{i,m}(t) + \mathbf{Q}_{i,i+1}^m \mathbf{A}_{i+1,m}(t)) \quad (22)$$

The definition of matrix $\mathbf{H}_{i,i-1}$, $\mathbf{H}_{i,i}$, $\mathbf{H}_{i,i+1}$ and vectors $\mathbf{Q}_{i,i-1}^m$, $\mathbf{Q}_{i,i}^m$, $\mathbf{Q}_{i,i+1}^m$ can be found in ref. [30].

Equation (22) contains 4 linear algebraic equations that relate the 12 boundary constants to the Fourier expansion coefficients. To determine the boundary constants, one has to apply equation (22), in turn, to each beam, resulting in a total of $4N$ equations as

$$\boldsymbol{\alpha}_i = \sum_{m=0}^{\infty} \tilde{\mathbf{H}}_i \bar{\mathbf{Q}}_i^m \mathbf{A}_{i,m}(t) \quad (23)$$

Making use of Eqs. (15) and (23), Eq. (10) can be expressed as

$$w_i(x,t) = \sum_{m=0}^{\infty} A_{i,m}(t) (\cos \lambda_{i,m} x + \boldsymbol{\zeta}_i(x)^T \tilde{\mathbf{H}}_i \bar{\mathbf{Q}}_i^m) + \sum_{\substack{j=1,N \\ j \neq i}} \sum_{m=0}^{\infty} A_{j,m}(t) \boldsymbol{\zeta}_j(x)^T \tilde{\mathbf{H}}_i \bar{\mathbf{Q}}_j^m \quad (24)$$

It should be noted that the boundary and coupling conditions, equations (2-9), have been explicitly used in establishing the relationship between the boundary constants in the polynomials and the Fourier expansion coefficients. Thus, the Fourier coefficients are now only required to satisfy the governing differential equation.

Substituting Eq. (24) into (1) and following the standard Galerkin procedure, one is able to obtain [30]

$$[\mathbf{K}_{pq}] \{\mathbf{A}_q\} + [\mathbf{M}_{pq}] \{\ddot{\mathbf{A}}_q\} = \{\mathbf{F}_p\} \quad (p, q = 1, 2, 3, \dots, N) \quad (25)$$

where

$$K_{pq,mm'} = \delta_{pq} (1 - \delta_{0m})(1 - \delta_{0m'}) (\delta_{mm'} + S_{p,m'm}^{pq}) \lambda_{pm'}^4 + \delta_{pq} \delta_{0m} \delta_{m0} S_{p,00}^{pq} + (1 - \delta_{pq}) \delta_{m0} S_{p,0m'}^{pq}, \quad (26)$$

$$\begin{aligned}
 M_{pq,mm'} &= \delta_{pq} (1 - \delta_{0m})(1 - \delta_{0m'}) (\delta_{mm'} + S_{p,mm'}^{pq} + S_{p,m'm}^{pq} + Z_{p,mm'}) + \\
 & \delta_{pq} \delta_{0m} \delta_{m0} (2 + Z_{p,00}^{pq}) + \delta_{pq} \delta_{0m'} (S_{p,m0}^{pq} + Z_{p,m0}^{pq}) + \delta_{pq} \delta_{m0} (S_{p,m'0}^{pq} + Z_{p,m'0}^{pq}) + \\
 & (1 - \delta_{pq})(1 - \delta_{0m})(S_{p,mm'}^{pq} + Z_{p,mm'}^{pq}) + (1 - \delta_{pq}) \delta_{m0} Z_{p,0m'}^{pq} \quad (27)
 \end{aligned}$$

and

$$f_{p,m} = 2/L_p \int_0^{L_p} \left(\cos \lambda_{pm} x + \zeta_p(x)^T \tilde{\mathbf{H}}_p \bar{\mathbf{Q}}_p^m \right) f_p(x - x_{fi}(t)) dx \quad (28)$$

for $m, m' = 0, 1, 2, 3, \dots$ and $p, q = 1, 2, 3, \dots, N$. Equation (25) represents a set of coupled second-order differential equations with respect to time which can be solved by direct numerical integration. In this study, the Newmark- β algorithm is used to perform the numerical integration.

3. RESULTS AND DISCUSSIONS

In order to validate the current model and analysis code, we will first consider a multi-span beam problem that was previously studied in ref. [4]. As illustrated in Fig. 2, this example involves a three-span stepped beam subjected to a single concentrated moving load. The relevant beam and material parameters are listed in Table 1. Under the current framework, this stepped continuous beam can be viewed as a collection of three separate beams that are rigidly coupled together. The continuous beam is assumed to be simply supported at its ends and the two join locations. The simply supported condition can be readily modeled by simply setting the stiffnesses of the (linear and rotational) coupling springs equal to infinity and zero, respectively.

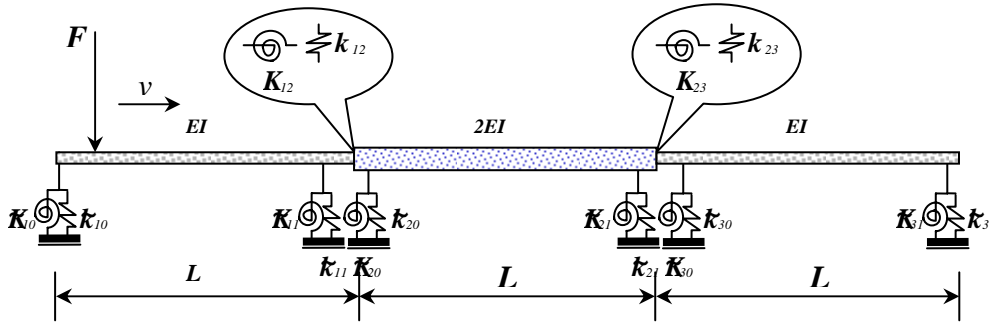


Figure 2. A three-span beam with non-uniform cross-section under a moving load.

The calculated natural frequencies for the first six modes are compared in Table 2 with those given in ref. [4]. Assume the beam is subjected to a point load, $F = 9.48 \times 10^3 N$, moving at two different (constant) speeds: $v = 35.57 m/s$. The corresponding deflections at the midpoint locations of the spans are plotted in Fig. 3. The results obtained by Henchi and Fafard [4] are also shown there for comparison. An excellent agreement is observed between these two sets of solutions. This problem was also studied by Dugush *et al.* [7] for different beam parameters and load profiles. It is here suffice to say that the current results also match closely with those given in ref. [7].

In a traditional multi-span beam problem, the beam displacement and its first derivative are both required to be continuous over the entire beam length. In many real-world applications, regardless of whether purposely or not, the joints between different spans cannot always be modeled as being infinitely rigid. Thus, the joint stiffnesses will actually constitute an additional set of model parameters, just like other beam and material variables, which may affect the response of a bridge to an applied load. While the effects of the beam parameters and loading conditions have been extensively studied, the impact of the coupling conditions on the dynamic response of a bridge was barely attempted before. Therefore, the following discussions will be primarily focused on the role of the coupling conditions.

Table 1. Beam and material properties.

Properties	Ref. [4]
L	20(m)
ρ	7800(Kg / m ³)
ρA	1000 (Kg / m)
EI	1.96×10^9 (Nm ²)
E	10.48×10^{10} (N / m ²)
F	9.48×10^3 (N)

Table 2. Comparison of natural frequencies.

Mode	Current	Ref. [4]
1	6.204	6.204
2	7.581	7.581
3	11.974	11.974
4	24.207	24.207
5	26.439	26.439
6	37.282	37.282

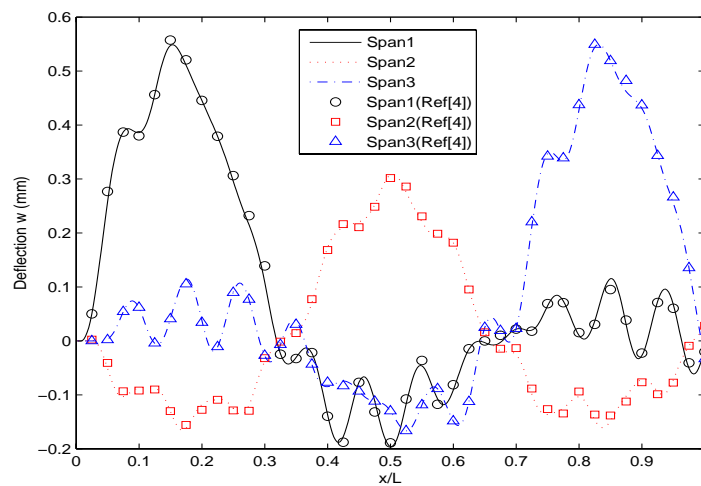


Figure 3. Flexural deflection at the midpoint of each span for $v = 35.57m/s$

As illustrated in Fig. 2, there are up to eight independent springs associated with each span in a general support/coupling configuration. Theoretically, each of these springs can be considered as an independent design variable, which makes it a formidable task to study a general case involving an arbitrary combination of these variables. For simplicity, we will only consider a slightly modified version of the above beam problem: the continuity requirement for the first derivative is relaxed at the locations of the two intermediate supports. In other words, two rotational springs, $K_{1,2}$ and $K_{2,3}$, of finite stiffness are now placed between the spans while the displacement is still assumed to be continuous over the entire length. Three different configurations are considered: 1) span 1 and 2 are elastically connected via a rotational spring while span 2 and 3 are rigidly coupled together (ER); 2) span 2 and 3 are elastically connected while span 1 and 2 are rigidly coupled together (RE); and 3) all three spans are elastically coupled together (EE). In all these cases, the rotational stiffness will vary between 10^6 and 10^{10} N/m.

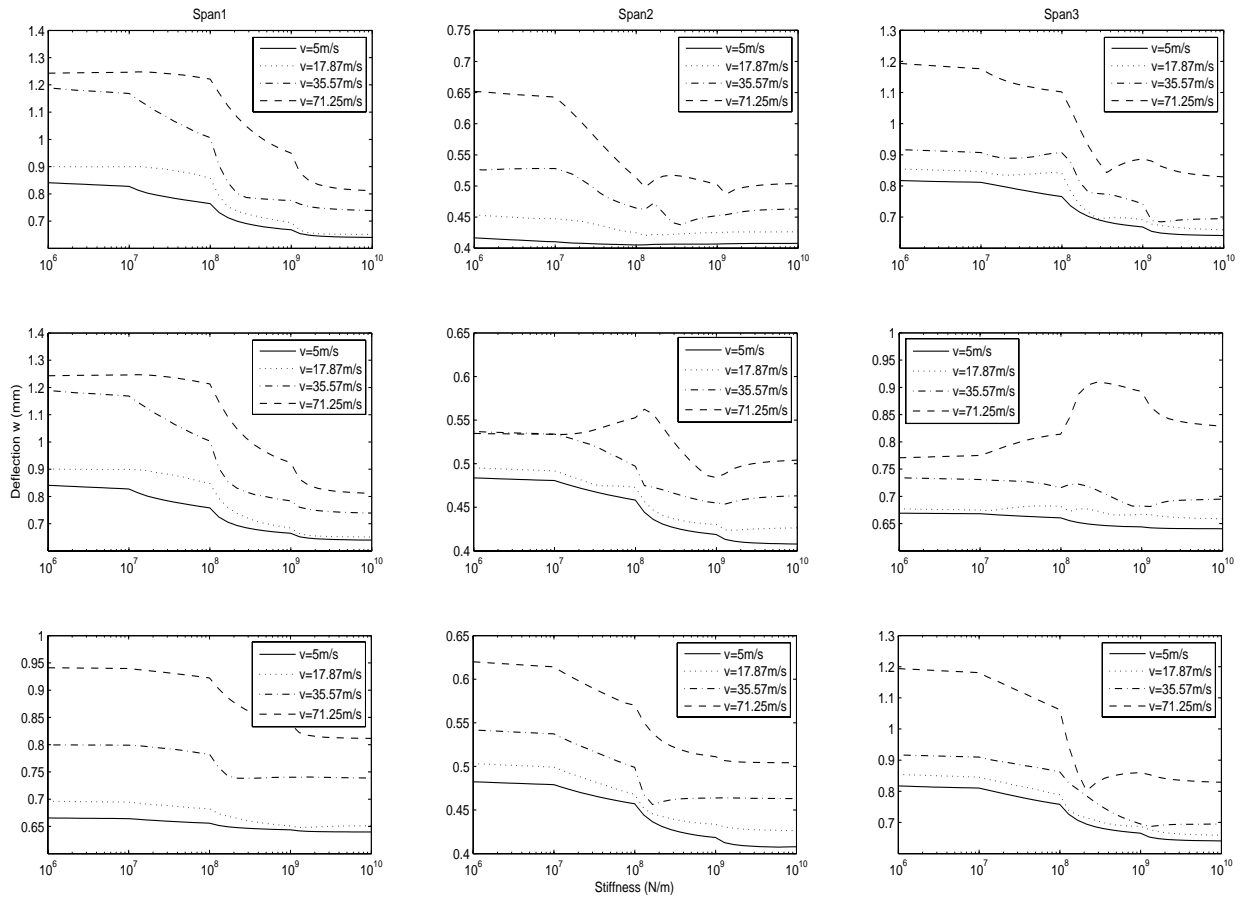


Figure 4. Peak-Peak deflection at the midpoint of each span for a few load profiles defined by a constant acceleration $a = 2 \text{ m/s}^2$ and different initial velocities: (i)-(iii) Elastic-Elastic; (iv)-(vi) Elastic-Rigid; (vii)-(ix) Rigid-Elastic.

The peak-peak value at the midpoint of each span is utilized to evaluate the dynamic behavior of the beam system. Figure 4 shows the peak-peak values vs. the stiffness of the coupling springs for a few different load profiles. It is seen that as the stiffness increases, the deflection at the midpoint of each span typically decreases until $K \cong 10^8$ (or $KL/EI \cong 1$).

The dynamic responses tend to exhibit a strong dependence on the coupling stiffness near this “critical” value. The peak-peak values typically increases with the traveling speed of the load for a given coupling stiffness and configuration.

From structural design point of view, a large variance in displacement implies that there is considerable room for modifying or improving the dynamic behavior of a bridge by varying the coupling stiffnesses. In bridge design, since the coupling conditions, unlike many other structural parameters, can be easily modified in a drastic manner, they may naturally constitute a set of design variables to be optimized for achieving a desired behavior of the bridge.

6. CONCLUSIONS

The vibration of a multi-span bridge subjected to a moving load has been investigated in a generic manner. Unlike in most multi-span bridge models, the displacement and its derivative are not here required to be continuous at the intermediate supports or any other locations. In other words, the joints between spans are now considered as a part of the design/model variables and can be modified or optimized for a desired dynamic behavior. In essence, the current model is a more general representation of multi-span bridges in which each span can be independently supported and arbitrarily coupled to its neighbors via a set of linear and rotational joints of any stiffness.

Since the traditional beam and material parameters have been extensively studied and well understood in regards to their effects on bridge vibration, this investigation is specifically focused on a set of rarely attempted model variables: the coupling conditions between the spans. It has been demonstrated through numerical examples that the coupling stiffness will generally have a direct and significant impact on the vibration on each span. In particular, the Peak-Peak deflection on a span is strongly dependent upon the coupling conditions local to that span, and fairly insensitive to the coupling conditions at distant junctions. For a given coupling arrangement, the Peak-Peak deflection on each span typically increases with the traveling speed of a concentrated load. Unlike other model variables, the coupling stiffness can vary easily by several orders of magnitude. It is found, however, that the dynamic behavior becomes particularly sensitive to the stiffness near a critical value defined by $KL/EI \cong 1$. Hence, the whole stiffness range can be practically compressed into a much smaller one bounded by what are respectively ten times smaller and larger than the critical value. Finally, a significantly large variance ratio for the deflection each span shall indicate certain room or a great potential for further improving bridge design through considering and optimizing the coupling conditions between spans. In general, there are up to eight independent (supporting and coupling) springs associated with each span. While this generalization makes the problem more complicated, it also opens more avenues for us to drastically improve the dynamic behavior of a multi-span bridge.

REFERENCES

1. J. Hino, T. Yoshimura and N. Ananthanarayana. A finite element method prediction of the vibration of a bridge subjected to a moving load. *Journal of Sound and Vibration* 96 (1984) 45-53.
2. M. Olsson. Finite Element, modal co-ordinate analysis of structures subjected to moving loads”, *Journal of Sound and Vibration* 99 (1985) 1-12.
3. Y. H. Lin and M. W. Trethewey. Finite element analysis of elastic beams subjected to moving dynamic loads. *Journal of Sound and Vibration* 136 (1990) 323-342.

4. K. Henchi and M. Fafard. Dynamic behavior of multi-span beams under moving loads. *Journal of Sound and Vibration* 199 (1997) 33-50.
5. R. T. Wang and J. S. Lin. Vibration of multi-span Timoshenko frames due to a moving load. *Journal of Sound and Vibration* 212 (1998) 417-434.
6. R. T. Wang and T. Y. Lin. Random vibration of multi-span Timoshenko beam due to a moving load. *Journal of Sound and Vibration* 213 (1998) 127-138.
7. Y. A. Dugush and M. Eisenberger. Vibrations of non-uniform continuous beams under moving loads. *Journal of Sound and Vibration*. 254 (2002) 911-926.
8. H. P. Lee. Dynamic response of a beam with intermediate point constraints subject to a moving load. *Journal of Sound and Vibration* 171 (1994) 361-368.
9. D. Y. Zheng, Y. K. Cheung, F. T. K. Au and Y. S. Cheng. Vibration of multi-span non-uniform beams under moving loads by using modified beam vibration functions. *Journal of Sound and Vibration* 212 (1998) 455-467.
10. H. P. Lee. Transverse vibration of a Timoshenko beam acted upon by an accelerating mass. *Applied Acoustics* 47 (1996) 319-330.
11. P. D. Cha. A general approach to formulating the frequency equations for a beam carrying miscellaneous attachments. *Journal of Sound and Vibration* 286 (2005) 921-939.
12. M. Ichikawa and Y. Miyakawa. Vibration Analysis of the Continuous Beam Subjected to a Moving Mass. *Journal of Sound and Vibration* 230 (2000) 493-506.
13. D. Y. Zheng, Y. K. Cheung, F. T. K. Au and Y. S. Cheng. Vibration of multi-span non-uniform beams under moving loads by using modified beam vibration functions. *Journal of Sound and Vibration* 212 (1998) 455-467.
14. Y. K. Cheung, F. T. K. Au, D. Y. Zheng and Y. S. Cheng. Vibration of multi-span non-uniform bridges under moving vehicles and trains by using modified beam vibration functions. *Journal of Sound and Vibration* 228 (1999) 611-628.
15. R. Hamada. Dynamic analysis of a beam under a moving force: a double Laplace transform solution. *Journal of Sound and Vibration* 74 (1981) 221-233.
16. R. P. Goel. Free vibrations of a beam-mass system with elastically restrained ends. *Journal of Sound and Vibration* 47 (1976) 9-14.
17. S.-W. Hong and J.-W. Kim. Modal analysis of multi-span Timoshenko beams connected or supported by resilient joints with damping. *Journal of Sound and Vibration* 227 (1999) 787-806.
18. T. P. Chang, F. I. Chang, M. F. Liu, On the eigenvalues of a viscously damped simple beam carrying point masses and springs. *Journal of Sound and Vibration* 240 (2001) 769-778.
19. E. H. Dowell. On some general properties of combined dynamical systems. *Journal of Applied Mechanics* 46 (1979) 206-209.
20. M. Gürgöze. On the alternative formulations of the frequency equation of a Bernoulli-Euler beam to which several spring-mass systems are attached in-span. *Journal of Sound and Vibration* 217 (1998) 585-595.
21. B. Posiada?a. Free vibrations of uniform Timoshenko beams with attachments. *Journal of Sound and Vibration* 204 (1997) 359-369.
22. J. W. Nicholson, L. A. Bergman. Free vibration of combined dynamical systems. *Journal of Engineering Mechanics*. 112 (1986) 1-13.
23. L. A. Bergman, D. M. McFarland, On the vibration of a point-supported linear distributed system, *ASME Journal of Vibration, Acoustics, Stress, and Reliability in Design*. 110 (1988) 485-592.
24. M. Abu-Hilal. Forced vibration of Euler-Bernoulli beams by means of dynamic Green functions. *Journal of Sound and Vibration* 267 (2002) 191-207.
25. S. Kukla. Application of Green functions in frequency analysis of Timoshenko beams with oscillators. *Journal of Sound and Vibration* 205 (1997) 355-363.
26. M. A. Foda and Z. Abduljabbar. A dynamic Green function formulation for the response of a beam structure to a moving mass. *Journal of Sound and Vibration* 210 (1998) 295-306.
27. W. L. Li. Free vibrations of beams with general boundary conditions. *Journal of Sound and Vibration* 237 (2000) 709-725.
28. W. L. Li, M. W. Bonilha and J. Xiao. Vibrations and power flow in a coupled beam system. *Proc. of IMECE2004*, Paper number: IMECE2004-59982.
29. W. L. Li, M. W. Bonilha and J. Xiao. Prediction of the Vibrations and Power Flows between Two Beams Connected at an Arbitrarily Angle. *Proc. of SAE Noise and Vibration Conference*, Traverse City, Michigan, 05NVC-222 (2005).
30. W. L. Li and Hongan Xu. A general Fourier series method for the vibration analysis of multi-span beam systems. submitted to *Journal of Structural Engineering*.